Significant enhancement of the power conversion efficiency for organic photovoltaic cells due to a P3HT pillar layer containing ZnSe quantum dots

Dae Hun Kim,[1] Young Hun Lee,[1] Dea Uk Lee,[1] Tae Whan Kim,[1,*] Sungwoo Kim,[2] and Sang Wook Kim[2]

[1]*Department of Electronics and Computer Engineering, Hanyang University, Seoul 133-791, Korea*
[2]*Department of Molecular Science and Technology, Ajou University, Suwon 443-749, Korea*
**twk@hanyang.ac.kr*

Abstract: High-efficiency organic photovoltaic (OPV) cells utilizing a poly(3-hexylthiophene) (P3HT) pillar layer containing ZnSe quantum dots (QDs) were fabricated by using a mixed solution method. Scanning electron microscopy and high-resolution transmission electron microscopy images showed that the ZnSe QDs were dispersed in the P3HT layer. The power conversion efficiency of the OPV cells with a P3HT pillar layer containing ZnSe QDs was as much as 100% higher than that of the OPV cells with a planar layer due to an enhancement of the photon-harvesting ability of the congregated P3HT particles containing ZnSe QDs and to an increase of the interfacial region for efficient charge transport.

OCIS codes: (040.0040) Detectors; (040.5350) Photovoltaic; (230.5590) Quantum-well, -wire and -dot devices.

References and links

1. Y. Kim, S. A. Choulis, J. Nelson, D. D. C. Bradley, S. Cook, and J. R. Durrant, "Device annealing effect in organic solar cells with blends of regioregular poly(3-hexylthiophene) and soluble fullerene," Appl. Phys. Lett. **86**(6), 063502 (2005).
2. J. Peet, J. Y. Kim, N. E. Coates, W. L. Ma, D. Moses, A. J. Heeger, and G. C. Bazan, "Efficiency enhancement in low-bandgap polymer solar cells by processing with alkane dithiols," Nat. Mater. **6**(7), 497–500 (2007).
3. J. S. Kim, J. H. Park, J. H. Lee, J. Jo, D. Y. Kim, and K. Cho, "Control of the electrode work function and active layer morphology via surface modification of indium tin oxide for high efficiency organic photovoltaics," Appl. Phys. Lett. **91**(11), 112111 (2007).
4. G. Dennler, M. C. Scharber, and C. J. Brabec, "Polymer-fullerene bulk-heterojunction solar cells," Adv. Mater. (Deerfield Beach Fla.) **21**(13), 1323–1338 (2009).
5. A. L. Ayzner, C. J. Tassone, S. H. Tolbert, and B. J. Schwartz, "Reappraising the need for bulk heterojunctions in polymer–fullerene photovoltaics: the role of carrier transport in all-solution-processed P3HT/PCBM bilayer solar cells," J. Phys. Chem. C **113**(46), 20050–20060 (2009).
6. K. H. Lee, P. E. Schwenn, A. R. G. Smith, G. Cavaye, P. E. Shaw, M. James, K. B. Krueger, I. R. Gentle, P. Meredith, and P. L. Burn, "Morphology of all-solution-processed 'Bilayer' organic solar cells," Adv. Mater. (Deerfield Beach Fla.) **23**(6), 766–770 (2011).
7. F. Yang, M. Shtein, and S. R. Forrest, "Controlled growth of a molecular bulk heterojunction photovoltaic cell," Nat. Mater. **4**(1), 37–41 (2005).
8. M. Aryal, K. Trivedi, and W. W. Hu, "Nano-confinement induced chain alignment in ordered P3HT nanostructures defined by nanoimprint lithography," ACS Nano **3**(10), 3085–3090 (2009).
9. J. Weickert, R. B. Dunbar, H. C. Hesse, W. Wiedemann, and L. Schmidt-Mende, "Nanostructured organic and hybrid solar cells," Adv. Mater. (Deerfield Beach Fla.) **23**(16), 1810–1828 (2011).
10. L. H. Nguyen, H. Hoppe, T. Erb, S. Günes, G. Gobsch, and N. S. Sariciftci, "Effects of annealing on the nanomorphology and performance of poly(alkylthiophene):fullerene bulk-heterojunction solar cells," Adv. Funct. Mater. **17**(7), 1071–1078 (2007).
11. R. A. Street and M. Schoendorf, "Interface state recombination in organic solar cells," Phys. Rev. B **81**(20), 205307 (2010).
12. A. A. Bakulin, J. C. Hummelen, M. S. Pshenichnikov, and P. H. M. van Loosdrecht, "Ultrafast hole-transfer dynamics in polymer/PCBM bulk heterojunctions," Adv. Funct. Mater. **20**(10), 1653–1660 (2010).
13. J. S. Kim, Y. Park, D. Y. Lee, J. H. Lee, J. H. Park, J. K. Kim, and K. Cho, "Poly(3-hexylthiophene) nanorods with aligned chain orientation for organic photovoltaics," Adv. Funct. Mater. **20**(4), 540–545 (2010).
14. F. A. Castro, H. Benmansour, C. F. O. Graeff, F. Nüesch, E. Tutis, and R. Hany, "Nanostructured organic layers via polymer demixing for interface-enhanced photovoltaic cells," Chem. Mater. **18**(23), 5504–5509 (2006).

#163114 - $15.00 USD Received 15 Feb 2012; accepted 19 Mar 2012; published 20 Apr 2012

15. C. Wu, Y. Zheng, C. Szymanski, and J. McNeill, "Energy transfer in a nanoscale multichromophoric system: fluorescent dye-doped conjugated polymer nanoparticles," J. Phys. Chem. C **112**(6), 1772–1781 (2008).
16. C. Wu, B. Bull, C. Szymanski, K. Christensen, and J. McNeill, "Multicolor conjugated polymer dots for biological fluorescence imaging," ACS Nano **2**(11), 2415–2423 (2008).
17. D. Tuncel and H. V. Demir, "Conjugated polymer nanoparticles," Nanoscale **2**(4), 484–494 (2010).
18. P. Brown and P. V. Kamat, "Quantum dot solar cells. Electrophoretic deposition of CdSe-C60 composite films and capture of photogenerated electrons with nC60 cluster shell," J. Am. Chem. Soc. **130**(28), 8890–8891 (2008).
19. F. Li, S. H. Cho, D. I. Son, T. W. Kim, S.-K. Lee, Y.-H. Cho, and S. Jin, "UV photovoltaic cells based on conjugated ZnO quantum dot/multiwalled carbon nanotube heterostructures," Appl. Phys. Lett. **94**(11), 111906 (2009).
20. D. I. Son, B. W. Kwon, J. D. Yang, D. H. Park, B. Angadi, and W. K. Choi, "High efficiency ultraviolet photovoltaic cells based on ZnO–C60 core–shell QDs with organic–inorganic multilayer structure," J. Mater. Chem. **22**(3), 816–819 (2011).
21. D. H. Kim, Y. P. Jeon, S. H. Lee, D. U. Lee, T. W. Kim, and S. H. Han, "Enhancement of the power conversion efficiency for organic photovoltaic devices due to an embedded rugged nanostructural layer," Org. Electron. (to be published).
22. M. C. Scharber, D. Mühlbacher, M. Koppe, P. Denk, C. Waldauf, A. J. Heeger, and C. J. Brabec, "Design rules for donors in bulk-heterojunction solar cells—towards 10% energy-conversion efficiency," Adv. Mater. (Deerfield Beach Fla.) **18**(6), 789–794 (2006).

1. Introduction

Photovoltaic cells have emerged as excellent candidates for their promising applications in renewable energy sources. Organic photovoltaic (OPV) cells have currently been receiving considerable attention due to their excellent advantages of high-mechanical flexibility, simple fabrication, and low cost [1–4]. The power conversion efficiency (PCE) of OPV cells with a bilayer heterojunction structure is currently over 5% [5,6] under a standard solar spectrum, AM1.5G, but enhancing their PCE is still necessary for practical mass applications. The prospect of potential applications of OPV cells has led to substantial research and development efforts to enhance the PCE of OPV cells, and OPV cells containing a nanostructural layer have been suggested to enhance the short-circuit current density (Jsc) and the PCE [7–9]. The increase in the charge separation in the active layer is attributed to an increase in the interfacial region between the donors and the acceptors [10–12], the P3HT chains of the nanostructural layer contain a partially-oriented face, resulting in enhanced charge mobility [13], and various process methods have been employed to reduce carrier recombination, resulting in an enhanced PCE for OPV cells [14–17]. Even though some studies on enhancing the PCE of OPV cells fabricated utilizing quantum dots (QDs) have been performed [18–20], the achievement of a high PCE for OPV cells is difficult due to the poor morphology of the active layer. While some studies concerning the fabrication and device characteristics of OPV cells containing poisonous CdSe QDs have been performed, works on the electrical characteristics of OPV cells containing environmentally-friendly ZnSe QDs have not been carried out yet. Furthermore, investigations on enhancing the PCE for OPV cells with an embedded rugged nanostructural layer containing QDs have not been conducted yet.

This letter reports data for a significant enhancement of the PCE for OPV cells due to a P3HT pillar layer containing ZnSe QDs. Absorbance measurements were performed to investigate the positions of the absorption peaks for P3HT and for ZnSe QDs. Atomic force microscopy (AFM) measurements were carried out to investigate the surface properties of a P3HT planar layer, a P3HT nanorod layer, and a P3HT pillar layer containing ZnSe QDs. Scanning electron microscopy (SEM) and high-resolution transmission electron microscopy (HRTEM) measurements were performed to investigate the microstructural properties of a P3HT pillar layer containing ZnSe QDs. Current density-voltage (J-V) measurements were performed to investigate the device performance of the OPV cells based on a P3HT planar layer, a P3HT nanorod layer, and a P3HT pillar layer containing ZnSe QDs.

2. Experimental details

The OPV cells used in this study were formed on indium-tin-oxide (ITO)-coated glass substrates, and the sheet resistance of the ITO thin film was approximately 10 Ω/sq. After the

#163114 - $15.00 USD Received 15 Feb 2012; accepted 19 Mar 2012; published 20 Apr 2012

surface of the chemically-cleaned ITO-coated glass substrates had been treated with an ultraviolet (UV)-ozone cleaner, the substrates were introduced into a glove box with a high-purity N_2 atmosphere. The poly (3,4-ethylenedioxythiophene):poly(styrenesulfonate) (PEDOT:PSS) layer was spin-coated onto the ITO-coated glass substrates by spin coating at 4500 rpm for 41 s in the glove box. Then, a 1-wt% P3HT solution was spin-coated onto the PEDOT:PSS layer at a spin coating speed of 2000 rpm for 60 s and was annealed at 145°C for 15 min. The solution for forming the nanorod film was prepared by using a mixed solution of 1 ml of 0.5-wt% P3HT and 0.1 ml of propylene glycol mono-methyl ether acetate (PGMEA) [21]. After the mixed solution had been sonicated for 15 min, the mixed solution was spin-coated onto the PEDOT:PSS layer at a spin rate of 4500 rpm for 36 s and was annealed at 145°C for 15 min. The blending solution for fabricating the P3HT pillar layer containing ZnSe QDs was prepared by using a mixed 1-wt% P3HT solution with a 10% volume ratio of PGMEA. The ZnSe QDs were added to the blending solution. After the blending solution containing ZnSe QDs had been sonicated for 10 min, the mixed solution was spin-coated onto the PEDOT:PSS layer at a spin coating speed of 2000 rpm for 60 s and was annealed at 145°C for 15 min. After the formation of the P3HT planar layer, the P3HT nanorod layer and the P3HT pillar layer, a C60 layer with a thickness of 40 nm was thermally evaporated in a vacuum chamber at a system pressure of approximately 8.5×10^{-7} Torr. Subsequently, the Liq cathode buffer layer was deposited on the active layer by using thermal evaporation; then, an Al layer with a thickness of 100 nm was formed. The active area of the fabricated cell was 2 mm × 2 mm.

Schematic diagrams of the fabricated Al/Liq/C60/P3HT/PEDOT:PSS/ITO cells with a nanorod layer and a pillar layer with ZnSe QDs are shown in Figs. 1(a) and 1(b), respectively. The thicknesses of the P3HT and the C60 layers shown in Fig. 1(a) are 40 and 40 nm, respectively. The thickness of the P3HT nanostructure layer in the OPV cells is 40 nm, as shown in Figs. 1(a) and 1(b). The AFM measurements were performed by using an XE-100 atomic force microscope, and the absorption measurements were carried out by using a Cary 100, UV-visible spectrometer. The HRTEM measurements were performed by using JEM-2100F, and the SEM measurements were carried out by using a JSM-6330F. The J-V curves were measured in the dark and under an illumination by using a Keithley 2400 source meter. The photovoltaic characteristics were measured under AM 1.5 simulated illumination with an intensity of 100 mW/cm^2.

#163114 - $15.00 USD Received 15 Feb 2012; accepted 19 Mar 2012; published 20 Apr 2012

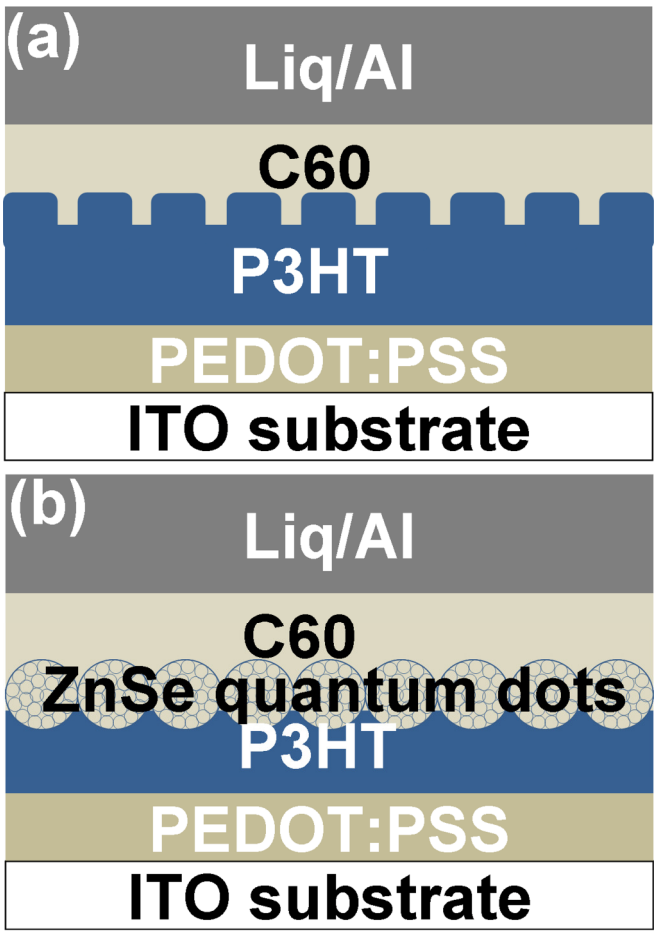

Fig. 1. Schematic diagrams of the solar cells utilizing (a) a P3HT nanorod layer and (b) a P3HT pillar layer containing ZnSe quantum dots.

3. Results and discussion

Figure 2 shows normalized absorption spectra of the ZnSe QDs and the P3HT layer formed on the glass substrates. The maximum absorbance peak for the P3HT layer appears at 520 nm. While the absorbance region of the organic materials dominantly appears between 500 and 600 nm in the visible region, that of ZnSe QDs appears in a broader wavelength range. The absorbance region of the ZnSe QDs appears at wavelengths blow 420 nm and covering the near-UV region. The P3HT pillar layer containing ZnSe QDs can absorb over a wide spectral range in the visible region and the near-UV region.

#163114 - $15.00 USD
Received 15 Feb 2012; accepted 19 Mar 2012; published 20 Apr 2012

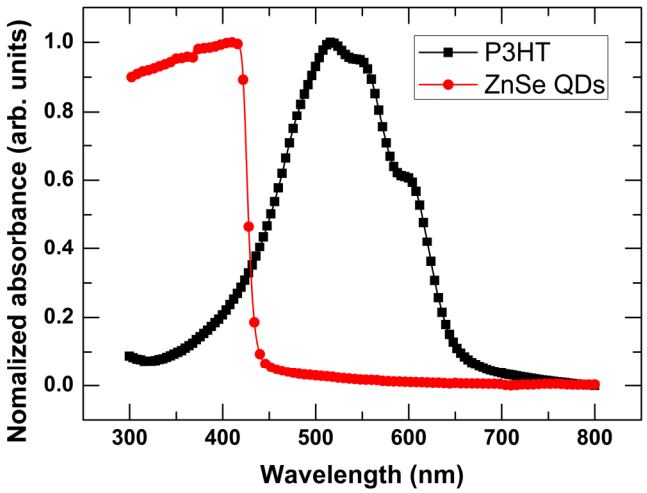

Fig. 2. Normalized absorption spectra of the ZnSe QDs and the P3HT layer formed on glass substrates.

Figure 3 shows (a) SEM and (b) HRTEM images for the congregated P3HT particles containing ZnSe QDs. The SEM image shows that the ZnSe QDs are dispersed in the congregated P3HT particles. The HRTEM image shows that the diameter of the nanocomposite consisting of the ZnSe QDs and the congregated P3HT particles is approximately 200 nm. The P3HT pillar layer with a triangular shape is formed due to a combination of congregated spherical P3HT particles containing ZnSe QDs and the P3HT layer formed by only P3HT molecular. The numbers of electrons and the holes in the active layer are increased due to the wide light absorption area of the ZnSe QDs.

#163114 - $15.00 USD
Received 15 Feb 2012; accepted 19 Mar 2012; published 20 Apr 2012

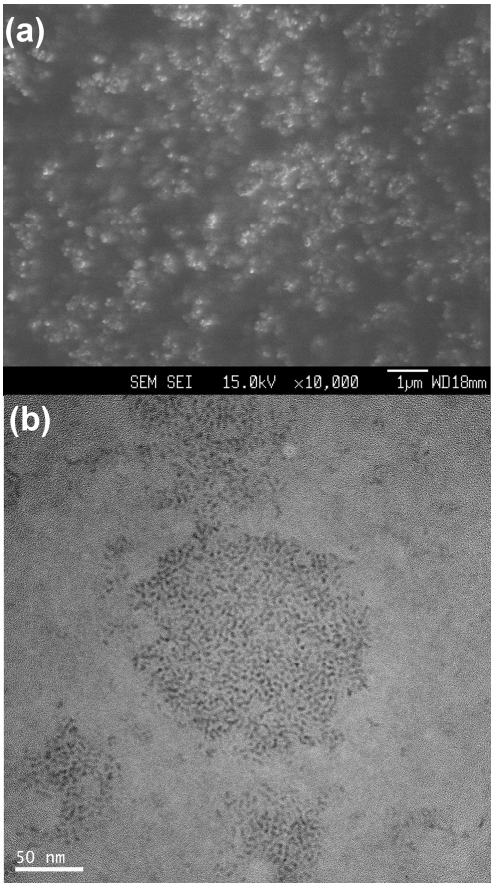

Fig. 3. (a) Scanning electron microscopy and (b) high-resolution transmission electron microscopy images of the P3HT particles containing ZnSe quantum dots.

Figure 4 shows AFM images and the corresponding AFM profile images of the P3HT planar layer, the P3HT nanorod layer, and the P3HT pillar layer containing ZnSe QDs. The AFM image for the P3HT planar layer shows that the root-mean-square average surface roughness of the P3HT planar layer is below 1 nm, as shown in Fig. 4(a). The AFM image shown in Fig. 4(b) shows that the P3HT layer consists of nanorods. The diameters of the nanorods are approximately 200 nm, and the lengths of the nanorods are between 30 and 40 nm. The surface area of the P3HT nanorods is much larger than that of the P3HT planar layer. The ZnSe QDs with a triangular pillar pattern are uniformly distributed, as shown in Fig. 3(b). The diameters of the triangular pillars are approximately 1 μm, and the lengths of the triangular pillars are 40 nm.

The PCE of the OPV cells with a nanostructure layer is higher than that of the OPV cells with a planar structure layer due to an enhancement of the efficiency for exciton dissociation and charge transport, as shown in Fig. 4. Because the charge separation in OPV cells increases with increasing area of the interface between the donor and the acceptor layers, the transport of the separated charges increases. Furthermore, the OPV cell with a nanostructural layer contains continuous paths along which charges can easily move, resulting in a decrease in charge recombination loss. When a C60 layer is thermally evaporated onto the P3HT nanorod layer, unoccupied regions can be formed in the interface between the P3HT nanorods and the C60 layer due to the shadow effect of the P3HT nanorods. The unoccupied regions, acting as charge traps, deteriorate the device performance. However, because the triangular P3HT pillars do not exhibit this shadow effect, the P3HT pillars can be conformally evaporated.

#163114 - $15.00 USD Received 15 Feb 2012; accepted 19 Mar 2012; published 20 Apr 2012

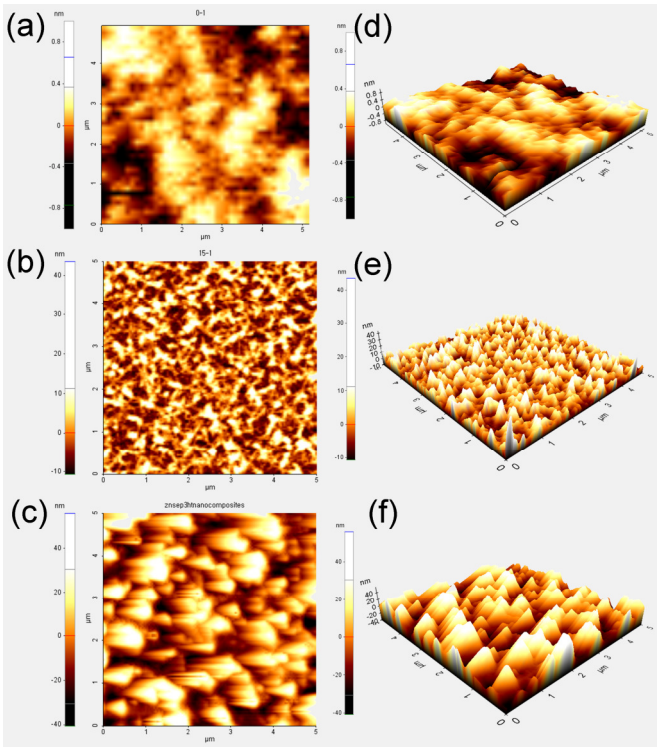

Fig. 4. Atomic force microscopy images of the (a) P3HT planar layer, (b) P3HT nanorod layer, and (c) P3HT pillar layer containing ZnSe quantum dots, and (d)-(f) corresponding profile images.

Figure 5(a) shows the J-V results for OPV cells fabricated utilizing a P3HT planar layer, a P3HT nanorod layer, and a P3HT nanopillar layer containing ZnSe QDs in the dark and under an AM 1.5 illumination at a power density of 100 mW/cm^2. Device performances of the OPV cells with a planar P3HT layer/C60 will be described elsewhere [21]. The PCE values of the OPV cells with planar P3HT layer/C60, P3HT nanorod layer/C60, and P3HT pillar layer containing ZnSe QDs/C60 structures were 0.8, 1.04, and 1.6%, respectively, and the corresponding Jsc values were 6.2, 8.3, and 8.6 mA/cm^2. The current density and the PCE of the OPV cells were increased due to an increase in the generation of charges caused by an increased quantity of photo-excitions at the P3HT layer containing ZnSe QDs, as shown in Fig. 2. The current density of OPV cells with a P3HT pillar layer is higher than that of OPV cells with a planar structure layer due to an increased generation of charges caused by enhanced photo-excitions at the congregated P3HT particles containing ZnSe QDs and due to an increase in the interface between the donor and the acceptor layers. Also, the enhancement of the PCE for the OPV cells with a P3HT pillar layer can be attributed to the conformal deposition on the P3HT pillar layer in Fig. 4. Figure 5(b) show that band diagram of OPV cells with a P3HT pillar layer containing ZnSe QDs. Because the conduction band edge of ZnSe QDs is higher than the highest occupied molecular orbital (HOMO) level of the P3HT layer, the open circuit voltage (V_{OC}) of the OPV cells is increased due to variations in V_{OC} resulting from the difference between the HOMO donor and the lowest occupied molecular orbital (LUMO) acceptor levels [22]. The V_{OC} values of the OPV cells with planar P3HT layer/C60, P3HT nanorod layer/C60, and P3HT pillar layer containing ZnSe QDs/C60 structures were 0.32, 0.31, and 0.35 V, respectively, and the corresponding fill factor (FF) values were 0.4, 0.38, and 0.53, respectively.

#163114 - $15.00 USD
Received 15 Feb 2012; accepted 19 Mar 2012; published 20 Apr 2012

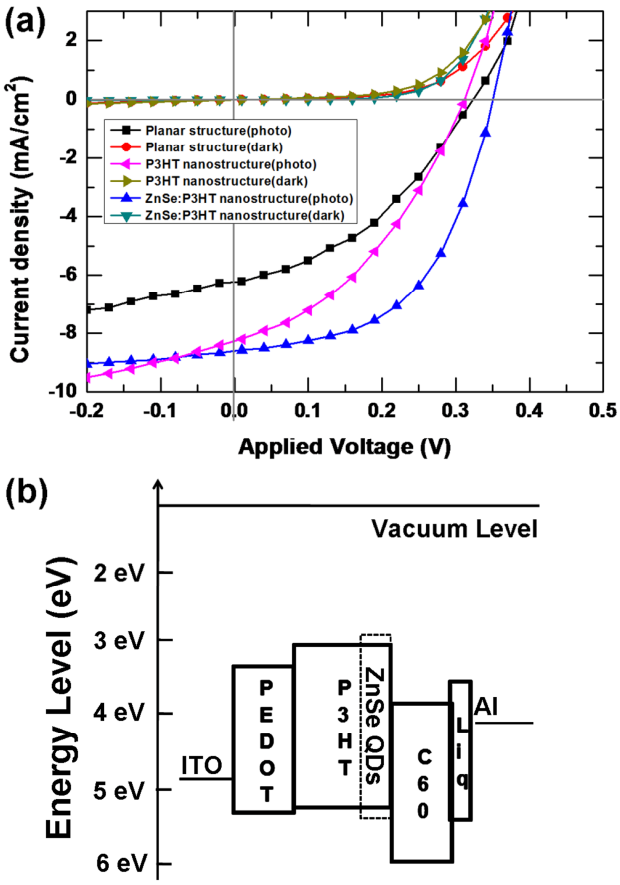

Fig. 5. (a) Current density-voltage curves of organic photovoltaic (OPV) cells with a P3HT planar layer, a P3HT nanorod layer, and a P3HT pillar layer containing ZnSe quantum dots in the dark and under an AM 1.5 illumination power density of 100 mW/cm^2. (b) Energy diagram of OPV cells with a P3HT pillar layer containing ZnSe quantum dots.

4. Summary and conclusions

OPV cells with a pillar layer containing ZnSe QDs, a nanorod layer, and a planar layer were fabricated utilizing a solution method. SEM and HRTEM images showed that the ZnSe QDs were dispersed in congregated P3HT particles. The PCE values of the OPV cells with a P3HT planar layer, a P3HT nanorod layer, and a P3HT pillar containing ZnSe QDs were 0.8, 1.04, 1.6%, respectively, and the corresponding Jsc magnitudes were 6.2, 8.3, and 8.6 mA/cm^2. The current density and the PCE of the OPV cells with a P3HT pillar layer containing ZnSe QDs were increased due to an enhanced photon-harvesting ability for the congregated P3HT particles containing ZnSe QDs and an increased interfacial region for efficient exciton separation. The V_{OC} and the FF values of the OPV cells with a P3HT pillar layer containing ZnSe QDs were increased even more due to the conformal deposition at the interface between the donor and the acceptor layers. The PCE of OPV cells with a pillar layer containing ZnSe QDs were as much as 100% higher than that of OPV cells with a planar layer.

Acknowledgments

This research was supported by Basic Science Research Program through the National Research Foundation of Korea (NRF) funded by the Ministry of Education, Science and Technology (2011-0025491).

#163114 - $15.00 USD Received 15 Feb 2012; accepted 19 Mar 2012; published 20 Apr 2012